Potential energy surface of HDO up to $25\,000\ \mathrm{cm}^{-1}$

S. N. Yurchenko, B. A. Voronin, R. N. Tolchenov, N. Doss, O. V. Naumenko, W. Thiel, and Jonathan Tennyson

Citation: J. Chem. Phys. **128**, 044312 (2008); doi: 10.1063/1.2806165
View online: https://doi.org/10.1063/1.2806165
View Table of Contents: http://aip.scitation.org/toc/jcp/128/4
Published by the American Institute of Physics

THE JOURNAL OF CHEMICAL PHYSICS **128**, 044312 (2008)

Potential energy surface of HDO up to 25 000 cm^{-1}

S. N. Yurchenko
Institut für Physikalische Chemie und Elektrochemie, Technische Universität Dresden, D-01062 Dresden, Germany

B. A. Voronin
Department of Physics and Astronomy, University College London, London, WC1E 6BT, United Kingdom and Institute of Atmospheric Optics, SB, Russian Academy of Sciences, Tomsk 634055, Russia

R. N. Tolchenov and N. Doss
Department of Physics and Astronomy, University College London, London WC1E 6BT, United Kingdom

O. V. Naumenko
Institute of Atmospheric Optics, SB, Russian Academy of Sciences, Tomsk 634055, Russia

W. Thiel
Max-Planck-Institut fur Kohlenforschung, Kaiser-Wilhelm-Platz 1, 45470, Mülheim an der Ruhr, Germany

Jonathan Tennyson[a)]
Department of Physics and Astronomy, University College London, London, WC1E 6BT, United Kingdom

(Received 30 May 2007; accepted 12 October 2007; published online 30 January 2008)

A new spectroscopically determined potential energy surface (PES) for HD^{16}O is presented. This surface is constructed by adjusting the high accuracy *ab initio* PES of Polyansky *et al.* [Science **299**, 539 (2003)] by fitting to both published experimental data and our still unpublished data. This refinement used experimentally derived term values up to 25 000 cm^{-1} and with $J \leqslant 8$: a data set of 3478 energy levels once some levels with ambiguous assignment is excluded. To improve the extrapolation properties of the empirical PES, the restraint that the resulting PESs remain close to the *ab initio* surface was imposed. The new HDO_07 PES reproduces the experimental data, including high J levels not included in the fit, with a root mean square error of 0.035 cm^{-1}. Predictions for rotation-vibration term values up to $J=12$ are made. © *2008 American Institute of Physics*. [DOI: 10.1063/1.2806165]

I. INTRODUCTION

The role of water vapor in the Universe and on Earth is unique. For example, $H_2{}^{16}O$ is the dominant absorber in the Earth's atmosphere. On earth, water consists of a number of isotopologues: $H_2{}^{16}O$ (0.997 317), $H_2{}^{18}O$ (0.001 999 83), $H_2{}^{17}O$ (0.000 372), HD^{16}O (0.000 310 69), HD^{18}O (0.000 000 623), HD^{17}O (0.000 000 116), and trace species such as HTO which are less important, where the numbers in parenthesis are the fractional abundance given by HITRAN-2004.[1] Given that the concentration of $H_2{}^{16}O$ in the Earth's atmosphere can ranges from $2\times10^{-6}\%$ to 5%,[2] the HD^{16}O concentration can be up to 0.0016%. HD^{16}O thus can be compared to CO_2 whose concentration is about 0.032%. It is therefore important not to neglect the influence of HD^{16}O, particularly because the absorption bands of HD^{16}O are strongly shifted from those of the symmetric H_2O isotopologues. Indeed, in many cases HD^{16}O absorption occurs in atmospheric windows and microwindows. The growing realization of the importance of weak water lines in climatic models points toward the use of comprehensive *ab initio* line lists rather than partial experimental compilations for such models.[3–5]

Determining the potential energy surface (PES) of a given molecule is an important task in chemical physics. For $H_2{}^{16}O$ many different PESs (Ref. 6–17) have been determined. Within the Born-Oppenheimer approximation these surfaces should also work for HD^{16}O. However, HD^{16}O shows strong non-Born-Oppenheimer effects,[18,19] and high accuracy work requires explicit treatment of HD^{16}O. Calculations on HD^{16}O are much less advanced than those on $H_2{}^{16}O$. Partridge and Schwenke[15] (PS) calculated HD^{16}O line positions and associated line intensities, up to 15 700 cm^{-1} using their spectroscopically determined PES and an *ab initio* dipole moment surface (DMS). This work was later improved by the same authors who used a significantly better DMS.[20,21] These calculations were repeated with better convergence by Tashkun and Tyuterev (spectra.iao.ru), who extended the range up to 17 800 cm^{-1}. However, experimental studies extend into the near ultraviolet,[22,23] and a number of problems remain at these higher frequencies.[24]

Nowadays, *ab initio* calculations can provide very accurate PES for small molecules. The water molecule is a prototypical example, see Ref. 25. The most accurate completely *ab initio* treatment of the rotation-vibration spectrum of HD^{16}O was performed as part of a systematic study aimed at obtaining the most accurate *ab initio* PES for all isotopologues of water.[26] This work, which resulted in the so-called

---

[a)] Author to whom correspondence should be addressed. Fax: +(44) 20 7679 7145. Electronic mail: j.tennyson@ucl.ac.uk.

CVRQD *ab initio* ground-state adiabatic PES,[27] has led directly to the most accurate equilibrium structure for water and its isotopologues,[28] and an improved dipole surface.[29] These studies form the starting point for the present work.

In this paper we report a spectroscopic potential energy surface of $HD^{16}O$ obtained by fitting to experimental term values. The corresponding fit has been restrained to remain close to the *ab initio* CVRQD PES. Previously this approach has been applied for constructing "spectroscopic" potentials of different systems,[30–33] but never using *ab initio* data of such high accuracy.

II. FITTING PROCEDURE

A. Refinement of the potential

Table I shows vibrational term values of $HD^{16}O$ computed using the *ab initio* CVRQD potential energy surface.[26,27] These are compared with the available experimental data, which are reproduced extremely well; the root-mean-square (rms) error for all the observed vibrational term values is less than 2 cm^{-1}. Similar results are obtained for rotational term values, see Table II, for an example. This *ab initio* PES, which is designed to cover the region up to 30 000 cm^{-1} above equilibrium, therefore provides a good starting approximation for an empirical improvement.

The *ab initio* CVRQD potential energy is given by Ref. 27 as

$$V = V_{\text{CBS}} + V_{\text{CV}} + V_{\text{MVD1}} + V_{\text{D2}} + V_{\text{Breit}} + V_{\text{QED}} + V_{\text{BODC}}, \tag{1}$$

where V_{CBS} represents the dominant complete basis set (CBS) extrapolation of the valence-only surface. The other terms represent the small corrections. These are the core-valence (V_{CV}), relativistic ($V_{\text{MVD1}}+V_{\text{D2}}+V_{\text{Breit}}$), Born-Oppenheimer diagonal (V_{BODC}), and quantum electrodynamic (V_{QED}) corrections, see Ref. 27 for further details. All these terms were used unaltered in the fit below. It should be noted that, unlike all other terms in the PES, the Born-Oppenheimer diagonal correction for $HD^{16}O$ has lower symmetry than that of $H_2{}^{16}O$,[18] and its inclusion is therefore vital for a proper treatment of HDO. The asymmetric terms were expressed using odd powers of the asymmetric stretch coordinate, s_2 below.

The V_{CBS} part was constructed as a CBS extrapolation from aug-cc-pV5Z and aug-cc-pV6Z multireference configuration interaction *ab initio* calculations[26,27] and was fitted using

$$V_{\text{CBS}}(r_1,r_2,\theta) = V^a(r_1) + V^a(r_2) + V^b(r_{\text{HH}}) + V^c(r_1,r_2,\theta), \tag{2}$$

where the two-body terms $V^a(r_1)$, $V^a(r_2)$ and $V^b(r_{\text{HH}})$ are given in Ref. 27 and the three-body term is written

$$V^c(r_1,r_2,\theta) = f_{000} + \left(\sum_{ijk}^{N_p} f_{ijk} s_1^i s_2^j s_3^k\right) \times \exp\{-\beta[(r_1-r_e)^2 + (r_2-r_e)^2]\}, \tag{3}$$

with j even and where

$$s_1 = (r_1+r_2)/2 - r_e, \tag{4}$$

$$s_2 = (r_1-r_2)/2, \tag{5}$$

$$s_3 = \cos\theta - \cos\theta_e, \tag{6}$$

and r_1, r_2, and θ denote the instantaneous values of the distances O–H and O–D and $\hat{\text{HOD}}$ bond angle, respectively; r_e, θ_e are their equilibrium values.

Here we utilize the polynomial coefficients f_{ijk} in Eq. (3) to modify the PES. These coefficients will be referred to as potential parameters below. The order of the polynomial, N_p used in the previous fit to the *ab initio* data[27] is 11 giving 113 parameters f_{ijk} which we vary in the fit. The nonlinear parameter β was frozen equal to 2.0 (Refs. 15 and 27) in all fits.

We impose an additional constraint requiring that the refined PES remains relatively close to the *ab initio* PES. By doing this we prevent our surface distorting into unrealistic shapes in regions not well characterized by the experimental data. Technically this is done by simultaneous fitting of the potential parameters f_{ijk} both to the observed data $E_l^{\text{obs.}}$ and to the *ab initio* energies V_m^{ai}. Here l is a short-hand notation for the rotation-vibration quantum numbers (J,K_a,K_c,v_1,v_2,v_3) and m denotes a geometry grid point. This approach has been discussed in details in Ref. 30 and is briefly outlined here. We note that the high quality of the starting potential and, in particular, the reliability with which it reproduces the observed equilibrium geometry[28] make it particularly appropriate for this approach.

Usually the available information on the *ab initio* energies does not sample all relevant geometries. Therefore, in practice, instead of using the original *ab initio* energies we prefer to deal with ersatz data, i.e., data generated using the analytical representation. Assuming that the CVRQD PES provides a reasonable description of the *ab initio* data in the spectroscopically important range of geometries, we generate a grid of potential energy points, here referred to as an *ab initio* PES. The grid consists of 2000 points covering the following geometries: $r_i(i=1,2)=0.85\ldots1.30$ Å and

TABLE I. Vibrational band origins in cm^{-1}: comparison with experiment and calculations using various PES [PS=Partridge and Schwenke, (Ref. 15), ai=*ab initio* CVRQD surface (Refs. 26 and 27)]. N gives the level number.

N	v_1	v_2	v_3	Obs.	Ref	Obs.-fit	Obs.-PS	Obs.-ai
2	0	1	0	1403.483 72	39	−0.013	−0.032	−0.323
3	1	0	0	2723.679 8	39	−0.030	0.020	0.363
4	0	2	0	2782.011 12	39	−0.003	−0.006	−0.558
5	0	0	1	3707.466 73	40	−0.004	−0.002	0.044
6	1	1	0	4099.955 9	40	−0.017	0.012	−0.239
7	0	3	0	4145.473 24	40	0.000	0.003	−0.581
8	0	1	1	5089.539 93	41	−0.002	0.009	−0.418
9	2	0	0	5363.824 46	41	−0.011	0.020	0.906
10	0	4	0	5420.041 8	45	0.045	0.089	−0.726
12	1	0	1	6415.460 62	38	−0.013	0.043	0.180
13	0	2	1	6451.899 2	38	−0.004	−0.007	−0.675
14	0	5	0	6690.413 2	47	−0.002	0.042	−1.063
15	2	1	0	6746.908 2	38	−0.000	−0.002	0.319
17	0	0	2	7250.519 21	38	0.025	−0.116	0.408
18	0	3	1	7754.605 5	58	−0.006	−0.015	−0.672
19	1	1	1	7808.758 6	58	0.008	0.038	−0.547
20	0	6	0	7914.317 0	58	−0.001	−0.046	−1.100
21	3	0	0	7918.171 9	58	0.006	0.040	1.103
26	2	0	1	9047.068 5	65	0.005	−0.027	0.378
28	1	2	1	9155.817 8	66	0.009	0.026	−0.838
29	3	1	0	9293.001 6	65	−0.033	−0.018	0.985
30	1	5	0	9381.786 1	65	0.008	0.201	−0.861
31	2	3	0	9487.915 3	65	0.008	−0.211	−0.779
32	0	2	2	9934.789	53	0.050	−0.016	0.068
33	1	0	2	9967.023	53	0.028	−0.074	0.083
36	4	0	0	10378.951 1	54	0.017	0.315	1.894
40	0	0	3	10631.683 2	54	0.010	−0.227	1.020
44	0	3	2	11242.923	53	0.029	−0.121	−0.508
45	1	1	2	11315.433 3	54	0.051	0.012	−0.092
48	2	2	1	11701.775 9	55	−0.002	0.054	−0.606
49	4	1	0	11754.581 8	55	−0.011	−0.041	0.795
50	1	7	0	11773.312 2	55	0.037	−0.120	−0.547
53	0	1	3	11969.753 0	57	0.003	−0.290	0.423
60	5	0	0	12767.141 5	57	−0.019	0.429	3.209
67	0	2	3	13278.350 8	57	0.010	−0.044	0.315
69	1	0	3	13331.606 1	57	0.014	−0.114	1.149
73	0	0	4	13853.628 0	57	−0.012	−0.250	1.901
87	1	1	3	14660.721 9	57	−0.000	−0.097	0.630
91	6	0	0	15065.712	49	0.006	0.750	4.140
93	0	1	4	15166.104 5	57	−0.000	−0.323	0.923
94	1	4	2	15170.951 0	57	0.002	−0.182	−0.019
115	0	2	4	16456.190 3	57	−0.013	0.199	0.927
125	0	0	5	16920.024 0	57	0.077	−0.032	3.105
152	0	1	5	18208.446 5	57	0.090	−0.161	2.448
190	0	0	6	19836.882 8	57	0.178	0.617	4.556
269	1	0	6	22454.468 8	57	−0.035	1.115	5.401
274	0	0	7	22625.528 5	57	0.004	1.645	6.008
371	1	0	7	25140.85	22 and 57	−0.113	2.421	6.746
					σ	0.039	0.479	1.867
					Δ(max)	0.178	2.421	6.746
					Δ(min)	−0.113	−0.324	−1.101

$\theta=60° \ldots 170°$. With these additional 2000 constraints all 113 f_{ijk} parameters are well defined independent of the number of experimental energies. Even in the extreme case of a single experimental energy, fitting all 113 parameters would still be well defined.

In the refinement, r_e and θ_e are kept fixed at 0.958 649 Å and 104.3475°. Required for efficient fitting are the first derivatives of the energies $E_l^{\text{calc.}}$ with respect to the fitting parameters. These are computed using the Hellmann-Feynman theorem,[34]

TABLE II. Rotational term values in cm^{-1} for $J=3$, $p=0$: comparison with experiment (Refs. 21, 22, 38, 48, 51, 52, 54, 57, 58, and 66) and calculations using various PES [PS=Partridge and Schwenke (Ref. 15), ai=*ab initio* CVRQD surface (Refs. 26 and 27)].

v_1	v_2	v_3	J	K_a	K_c	Obs.	Obs.-fit	Obs.-PS	Obs.-ai
0	0	0	3	0	3	91.3302	0.005	−0.005	0.004
0	0	0	3	1	3	100.3909	0.004	−0.004	0.002
0	0	0	3	2	1	157.0647	0.006	−0.001	0.000
0	0	0	3	3	1	233.0237	0.005	0.004	−0.007
0	1	0	3	0	3	1 495.0554	−0.009	−0.037	−0.318
0	1	0	3	1	3	1 505.5930	−0.010	−0.035	−0.321
0	1	0	3	2	1	1 569.0241	−0.010	−0.032	−0.323
0	1	0	3	3	1	1 654.6585	−0.011	−0.023	−0.331
1	0	0	3	0	3	2 813.4421	−0.028	0.018	0.368
1	0	0	3	1	3	2 822.6696	−0.028	0.016	0.367
0	2	0	3	0	3	2 873.8325	−0.000	−0.008	−0.554
1	0	0	3	2	1	2 879.1657	−0.026	0.012	0.370
0	2	0	3	1	3	2 886.2799	−0.001	−0.006	−0.560
1	0	0	3	3	1	2 954.9264	−0.024	0.006	0.364
0	2	0	3	2	1	2 957.5142	−0.002	−0.003	−0.569
0	2	0	3	3	1	3 054.9334	−0.005	0.005	−0.579
0	0	1	3	0	3	3 798.0644	−0.002	−0.008	0.048
0	0	1	3	1	3	3 806.1046	−0.003	−0.005	0.045
0	0	1	3	2	1	3 860.2436	−0.004	−0.001	0.043
0	0	1	3	3	1	3 931.1395	−0.009	0.011	0.033
1	1	0	3	0	3	4 190.6668	−0.010	0.011	−0.221
1	1	0	3	1	3	4 203.3774	−0.012	0.009	−0.185
0	3	0	3	0	3	4 236.9038	−0.000	0.004	−0.594
0	3	0	3	1	3	4 250.2713	0.000	0.005	−0.631
1	1	0	3	2	1	4 272.3667	−0.016	0.002	−0.082
0	3	0	3	2	1	4 326.4944	0.004	0.012	−0.733
1	1	0	3	3	1	4 361.5094	−0.016	−0.009	−0.031
0	3	0	3	3	1	4 435.7961	0.003	0.022	−0.787
0	1	1	3	0	3	5 180.4043	−0.002	0.005	−0.415
0	1	1	3	1	3	5 189.7376	−0.003	0.008	−0.415
0	1	1	3	2	1	5 250.1646	−0.005	0.013	−0.413
0	1	1	3	3	1	5 329.9146	−0.008	0.027	−0.412
2	0	0	3	0	3	5 451.9209	−0.012	0.021	0.909
2	0	0	3	1	3	5 461.0830	−0.011	0.017	0.908
0	4	0	3	0	3	5 511.8403	0.012	0.051	−0.752
2	0	0	3	2	1	5 516.4914	−0.006	0.008	0.904
0	4	0	3	1	3	5 530.7072	0.011	0.055	−0.727
2	0	0	3	3	1	5 591.3286	−0.000	−0.010	0.896
1	2	0	3	0	3	5 597.1042	−0.005	−0.017	−0.643
1	2	0	3	1	3	5 610.8462	−0.004	−0.019	−0.667
0	4	0	3	2	1	5 621.7275	−0.002	0.054	−0.617
1	2	0	3	2	1	5 687.8415	−0.001	−0.023	−0.775
0	4	0	3	3	1	5 802.9271	0.002	−0.006	−0.939
1	0	1	3	0	3	6 504.7706	−0.014	0.039	0.195
1	0	1	3	1	3	6 513.3678	−0.016	0.037	0.212
0	2	1	3	0	3	6 542.8009	−0.009	−0.008	−0.686
0	2	1	3	1	3	6 553.4447	−0.010	−0.005	−0.704
1	0	1	3	2	1	6 568.6409	−0.017	0.031	0.266
0	2	1	3	2	1	6 619.9010	−0.013	0.004	−0.759
1	0	1	3	3	1	6 640.3897	−0.023	0.026	0.284
0	2	1	3	3	1	6 709.5727	−0.018	0.017	−0.783
0	5	0	3	0	3	6 782.6131	−0.002	0.044	−1.046
0	5	0	3	1	3	6 808.7812	−0.011	0.053	−0.936
2	1	0	3	0	3	6 835.4072	0.002	−0.001	0.306
2	1	0	3	1	3	6 847.1741	0.009	−0.005	0.230
2	1	0	3	2	1	6 902.1695	−0.023	0.000	0.283
0	5	0	3	2	1	6 932.1680	0.017	0.061	−0.878
1	3	0	3	0	3	6 940.3790	0.001	−0.042	−0.825
1	3	0	3	1	3	6 955.7465	0.001	−0.054	−0.835

TABLE II. (*Continued.*)

v_1	v_2	v_3	J	K_a	K_c	Obs.	Obs.-fit	Obs.-PS	Obs.-ai
2	1	0	3	3	1	6 989.7789	0.000	−0.039	0.440
0	0	2	3	0	3	7 340.3550	0.025	−0.122	0.414
0	0	2	3	1	3	7 347.4214	0.024	−0.118	0.411
0	0	2	3	2	1	7 399.1278	0.023	−0.113	0.410
0	0	2	3	3	1	7 465.0669	0.018	−0.097	0.402
0	3	1	3	0	3	7 845.2879	−0.001	−0.012	−0.648
0	3	1	3	1	3	7 857.8590	−0.002	−0.008	−0.610
1	1	1	3	0	3	7 898.9510	0.005	0.036	−0.565
1	1	1	3	1	3	7 909.8400	0.005	0.037	−0.604
1	1	1	3	2	1	7 928.5830	−0.001	0.010	−0.432
0	3	1	3	2	1	7 977.5270	0.001	0.031	−0.776
3	0	0	3	0	3	8 004.2490	−0.001	0.056	1.453
0	6	0	3	0	3	8 007.4630	0.005	−0.051	−1.442
3	0	0	3	1	3	8 013.5500	0.001	0.049	1.554
1	1	1	3	3	1	8 017.0379	−0.005	0.029	−0.237
3	0	0	3	2	1	8 067.9590	0.007	0.034	1.550
0	3	1	3	3	1	8 073.9264	−0.006	0.024	−0.957
3	0	0	3	3	1	8 142.0180	0.019	0.006	1.538
2	2	0	3	0	3	8 178.9222	−0.001	0.109	−0.209
0	1	2	3	0	3	8 701.2180	0.019	−0.134	−0.145
0	1	2	3	1	3	8 709.3850	0.014	−0.135	−0.146
0	1	2	3	2	1	8 766.8870	0.010	−0.133	−0.141
0	1	2	3	3	1	8 840.8180	−0.001	−0.128	−0.137
2	0	1	3	0	3	9 135.1428	−0.012	−0.071	0.141
2	0	1	3	1	3	9 139.0860	0.001	0.022	0.531
1	4	0	3	1	3	9 156.9426	−0.000	−0.110	−0.922
2	0	1	3	2	1	9 193.8659	0.004	0.036	0.744
0	7	0	3	1	3	9 240.8755	0.015	−0.152	−1.415
1	2	1	3	0	3	9 245.9402	0.006	0.017	−0.895
0	4	1	3	2	1	9 250.0251	0.015	−0.044	−1.023
1	2	1	3	1	3	9 261.1900	−0.000	0.052	−1.175
2	0	1	3	3	1	9 264.7782	−0.000	0.021	0.749
1	2	1	3	2	1	9 327.6882	−0.003	−0.009	−0.887
0	4	1	3	3	1	9 362.2007	0.003	−0.006	−0.800
3	1	0	3	0	3	9 379.5485	−0.033	−0.012	0.987
3	1	0	3	1	3	9 390.0872	−0.027	−0.023	0.994
1	2	1	3	3	1	9 428.6308	−0.005	−0.008	−1.048
0	7	0	3	2	1	9 446.3477	−0.045	0.023	−0.724
3	1	0	3	2	1	9 452.6210	−0.008	−0.047	0.054
0	5	1	3	0	3	9 472.1227	0.014	0.206	−0.855
0	5	1	3	1	3	9 495.2708	0.014	0.200	−0.797
3	1	0	3	3	1	9 533.7054	0.005	−0.075	1.025
2	3	0	3	0	3	9 578.3412	−0.005	−0.195	−0.787
2	3	0	3	2	1	9 596.5589	0.047	0.165	−0.639
2	3	0	3	3	1	9 735.4903	0.020	0.017	−0.872
0	2	2	3	0	3	10 024.3050	0.033	−0.035	0.098
0	2	2	3	1	3	10 032.9500	0.025	−0.043	0.145
1	0	2	3	0	3	10 056.2540	0.013	−0.082	0.036
1	0	2	3	1	3	10 064.4230	0.012	−0.080	−0.013
1	0	2	3	2	1	10 090.3360	0.026	−0.045	0.408
0	2	2	3	2	1	10 122.7570	0.007	−0.073	−0.266
1	0	2	3	3	1	10 160.5680	0.025	−0.044	0.608
0	2	2	3	3	1	10 202.1460	0.013	−0.052	−0.441
4	0	0	3	0	3	10 464.5207	0.017	0.314	1.971
4	0	0	3	1	3	10 474.2346	0.018	0.298	1.957
4	0	0	3	2	1	10 532.2193	0.024	0.082	0.689
4	0	0	3	3	1	10 602.5402	0.020	0.231	2.173
0	0	3	3	0	3	10 720.7236	0.005	−0.233	1.025
0	0	3	3	1	3	10 726.8779	0.005	−0.229	1.023
0	0	3	3	2	1	10 776.2778	0.003	−0.223	1.022

TABLE II. (*Continued.*)

v_1	v_2	v_3	J	K_a	K_c	Obs.	Obs.-fit	Obs.-PS	Obs.-ai
0	0	3	3	3	1	10 837.3960	0.000	−0.208	1.021
0	3	2	3	0	3	11 333.2500	0.017	−0.136	−0.508
0	3	2	3	1	3	11 344.6030	0.027	−0.127	−0.478
1	1	2	3	0	3	11 404.4839	0.027	−0.008	−0.123
1	1	2	3	1	3	11 413.0864	0.009	−0.034	−0.167
0	3	2	3	2	1	11 415.0580	0.026	−0.115	−0.342
1	1	2	3	2	1	11 473.7583	0.027	0.009	−0.241
0	3	2	3	3	1	11 503.4280	0.018	−0.129	−0.117
1	1	2	3	3	1	11 555.6234	−0.000	−0.006	−0.467
3	0	1	3	2	1	11 729.6996	−0.004	0.113	1.394
2	2	1	3	0	3	11 791.2997	−0.003	0.051	−0.644
3	0	1	3	3	1	11 800.2949	−0.002	0.085	1.389
1	2	2	3	1	3	11 807.1127	0.007	0.124	−0.438
4	1	0	3	0	3	11 841.1677	−0.027	−0.038	1.031
4	1	0	3	1	3	11 854.2191	−0.021	−0.049	1.340
0	7	1	3	0	3	11 862.1391	0.034	−0.129	−0.717
1	2	2	3	2	1	11 883.2104	0.004	0.147	−0.143
4	1	0	3	2	1	11 916.6372	−0.003	−0.096	1.308
0	6	1	3	3	1	11 954.1591	−0.004	0.098	−0.772
4	1	0	3	3	1	12 005.8296	0.025	−0.109	0.186
0	3	3	3	0	3	12 045.8520	−0.041	0.307	−0.163
0	1	3	3	0	3	12 059.1114	0.004	−0.291	0.429
0	3	3	3	1	3	12 065.6857	−0.009	0.126	0.173
0	1	3	3	1	3	12 066.4296	−0.000	−0.173	0.086
0	1	3	3	2	1	12 120.9352	0.005	−0.282	0.452
0	1	3	3	3	1	12 189.2536	0.003	−0.268	−0.287
5	0	0	3	0	3	12 850.3230	−0.035	0.426	3.201
5	0	0	3	1	3	12 859.5210	−0.031	0.410	3.176
5	0	0	3	2	1	12 912.4210	−0.022	0.390	3.196
5	0	0	3	3	1	12 985.4380	−0.002	0.342	3.190
0	2	3	3	0	3	13 367.7760	0.015	−0.043	0.336
0	2	3	3	1	3	13 375.9100	0.025	−0.034	0.370
1	0	3	3	0	3	13 419.4122	0.000	−0.110	1.135
1	0	3	3	0	3	13 425.8446	0.000	−0.122	−1.636
0	2	3	3	2	1	13 435.1990	0.017	−0.048	0.512
1	0	3	3	2	1	13 476.6220	0.007	−0.101	0.997
0	2	3	3	3	1	13 508.0270	0.028	−0.045	0.834
1	0	3	3	3	1	13 541.9790	0.009	−0.076	0.728
0	0	4	3	0	3	13 941.8550	−0.014	−0.243	−0.140
0	0	4	3	1	3	13 947.1470	−0.025	−0.253	1.904
0	0	4	3	2	1	13 994.3860	−0.031	−0.254	1.908
0	0	4	3	3	1	14 050.8360	−0.025	−0.232	0.534
5	1	0	3	0	3	14 231.1411	0.058	0.025	0.362
1	1	3	3	0	3	14 748.8846	−0.005	−0.100	0.617
1	1	3	3	1	3	14 756.2989	0.005	−0.084	0.623
1	1	3	3	2	1	14 811.9619	0.001	−0.072	0.577
1	1	3	3	3	1	14 883.5539	0.019	−0.017	0.494
6	0	0	3	1	3	15 156.6430	−0.018	0.730	1.293
6	0	0	3	2	1	15 208.6660	−0.020	0.693	4.095
0	1	4	3	0	3	15 254.2090	−0.007	−0.270	0.573
0	12	0	3	0	3	15 256.8950	−0.003	−0.198	−1.147
1	4	2	3	0	3	15 260.2580	0.012	−0.165	0.034
0	1	4	3	1	3	15 262.2100	−0.014	−0.340	0.244
1	4	2	3	1	3	15 273.7840	0.027	−0.062	−0.504
6	0	0	3	3	1	15 281.1967	0.031	0.675	4.135
0	1	4	3	2	1	15 314.4230	−0.013	−0.371	1.349
0	1	4	3	3	1	15 377.410	−0.013	−0.354	1.394
0	2	4	3	0	3	16 544.4225	0.061	0.133	0.886
1	11	0	3	0	3	16 545.8141	0.092	0.112	−1.158
0	2	4	3	1	3	16 551.8910	0.001	0.191	1.015

TABLE II. (*Continued.*)

v_1	v_2	v_3	J	K_a	K_c	Obs.	Obs.-fit	Obs.-PS	Obs.-ai
0	2	4	3	2	1	16 608.6161	0.019	0.161	1.261
1	0	4	3	0	3	16 625.8680	0.028	−0.034	0.962
1	0	4	3	1	3	16 631.2440	0.004	−0.049	2.290
0	2	4	3	3	1	16 678.0171	0.006	0.089	1.961
1	0	4	3	2	1	16 679.260	0.020	0.050	1.738
1	0	4	3	3	1	16 735.9480	−0.032	−0.063	2.119
0	0	5	3	0	3	17 007.3890	0.053	−0.037	3.111
0	0	5	3	1	3	17 011.8740	0.052	−0.035	3.110
0	0	5	3	2	1	17 057.0270	0.048	−0.030	3.119
0	0	5	3	3	1	17 108.8567	0.043	−0.017	3.129
0	0	5	3	3	1	17 108.8570	−0.091	−0.471	−1.068
0	1	5	3	0	3	18 296.2232	0.031	−0.172	0.876
0	1	5	3	1	3	18 301.2369	0.090	−0.184	2.551
0	1	5	3	2	1	18 350.9750	0.081	−0.176	2.084
0	1	5	3	3	1	18 408.5688	0.067	0.184	2.075
1	0	5	3	0	3	19 670.4467	0.052	0.253	2.679
1	0	5	3	1	3	19 675.0639	0.060	0.262	3.777
1	0	5	3	2	1	19 720.1666	0.051	0.248	3.749
0	0	6	3	0	3	19 923.3875	0.148	0.614	4.555
0	0	6	3	1	3	19 927.1417	0.145	0.617	4.549
0	0	6	3	2	1	19 970.3249	0.141	0.623	4.574
0	0	6	3	3	1	20 017.6625	0.129	0.642	4.068
0	0	7	3	0	3	22 711.1709	−0.011	1.630	5.959
0	0	7	3	1	3	22 714.3285	−0.017	1.630	5.952
0	0	7	3	2	1	22 755.750	−0.024	1.645	5.987
0	0	7	3	3	1	22 799.167	−0.052	1.663	6.020
1	0	7	3	0	3	25 225.26	−0.023	2.441	6.568
1	0	7	3	1	3	25 228.39	0.115	−1.418	−2.860
				σ			0.031	0.347	1.563
				Δ(max)			0.148	2.441	6.568
				Δ(min)			−0.092	−1.418	−2.860

$$\frac{\partial E_l}{\partial f_{ijk}} = \langle \Psi_l | \frac{\partial H_{\mathrm{rv}}(f_{ijk})}{\partial f_{ijk}} | \Psi_l \rangle = \langle \Psi_l | s_1^i s_2^j s_3^k \exp\{-\beta[(r_1 - r_e)^2 + (r_2 - r_e)^2]\} | \Psi_l \rangle, \tag{7}$$

where H_{rv} is the rotation-vibration Hamiltonian and Ψ_l is the eigenfunction corresponding to the eigenvalue E_l. In Eq. (7) we use the fact that the Hamiltonian (and the potential energy function) is a linear function of f_{ijk}. The derivatives (gradients) of the potential energy function are computed using the finite difference method. The three-dimensional integration implied by Eq. (7) is performed numerically.[35]

B. Nuclear motion procedure

All rotation-vibration calculations were performed using the DVR3D program suite[35] in Radau coordinates. The discrete variable representation (DVR) grid in the angular coordinate is based on (associated) Legendre polynomials, while the radial grid points are set up using Morse oscillatorlike functions[36] as the underlying basis sets. The functions are defined in terms of parameters, r_e, ω_e, and D_e.[35]

In contrast with $H_2{}^{16}O$, $HD^{16}O$ requires not three, but six Morse oscillator parameters to be determined: three for the OH bond and three for the OD bond. To determine these parameters we fixed three for one bond and made a series of calculations varying the other three, mainly r_e and ω_e to which the results are particularly sensitive. After finding parameters which minimize the energies of the states below 25 000 cm^{-1}, the procedure was repeated for the parameters of the other bond. The set of parameters giving the best result was $r_e = 2.05a_0$, $\omega_e = 0.0078$ a.u., and $D_e = 0.20E_h$ for OH and $r_e = 1.82a_0$, $\omega_e = 0.0081$ a.u., and $D_e = 0.18E_h$ for OD. Their values agree well with those optimized for calculations on $H_2{}^{16}O$ for a similar energy range.[37]

The final DVR grid used was given by 30 points in each of the two radial coordinates and 48 (associated)-Gauss-Legendre points in the angular coordinate. The convergence of this grid was determined by tests performed for calculations with $J = 0$, 3, and 10; we also checked agreement with experimental data up to 25 000 cm^{-1}.[22] A final vibrational Hamiltonian of dimension of 4000 was used for all calculations reported below. For levels below 24 000 cm^{-1} this is sufficient to get well converged results; above this convergence errors of about 0.1 cm^{-1} are found up to 24 000 cm^{-1}, and more above that energy.

DVR3D has options to embed the body-fixed z axis along the Radau coordinate approximating either the OH or the OD bond.[35] Tests showed that embedding this axis close to the OH bond gave faster convergence for rotationally excited states. For these calculations we used a basis of $1500\times(J+1-p)$ functions taken from the first step of the calculation,[35] where $(-1)^{J+p}$ gives the parity. This basis gave good convergence for $J=3$ levels up to 25 500 cm^{-1} and $J=10$ levels up to 23 000 cm^{-1}, which is sufficient for the fit.

At high levels of excitation it is not always readily apparent what the correct vibrational quantum numbers are for a particular state. Initial vibrational quantum numbers were selected using the overlap of the wave function with a simple product of one-dimensional functions generated from cuts through the PES which pass through the equilibrium geometry. Using this method each state was given a unique label although in practice there is some ambiguity about labeling some of the higher lying states.

C. Experimental data

An important preliminary task for the spectroscopic determination of a PES is to collect the available experimental data. Here we attempted to use all published data plus some of our own unpublished results.

For energy levels below 8000 cm^{-1} we use all the data made available electronically by Toth.[38] These data come from a series of papers by Toth and co-workers[39–44] and span levels of the vibrational states (000), (010), (100), (020), (001), (110), (030), (011), (120), (021), (200), (101), (210), and (002). Further data, including the band origin of (040), were taken from Parekunnel *et al.*[45] Finally energy levels from the weak (050) and (130) bands were taken from Ulenikov *et al.*[46] and Macko *et al.*[47]

In the near infrared and visible region there are series of long path length studies by Campargue and co-workers,[48–55] that mostly used intracavity laser absorption spectroscopy (ICLAS). This work contains assignments to about 30 vibrational bands, including the highest bending state (0 12 0) so far observed for any isotopologue of H_2O. These ICLAS studies are deep, that is, probe very low intensity transitions, but only cover very limited wavelength ranges.

More comprehensive spectra have been recorded using Fourier transform spectrometers.[23,56] Here we use data from our recent (re-)assignment of these spectra[57] which cover an extended region from 11 500 to 23 000 cm^{-1}. We also used a series of near infrared studies by Hu and co-workers.[58–60]

The highest $HD^{16}O$ energy levels studied to date are by Theule *et al.*,[22] who used a two photon technique[61] to probe levels at about 25 140 cm^{-1}. We recently showed that these levels belong to the (107) vibrational state.[57]

Finally (050)-(000) transitions of $HD^{16}O$ in region of 6000–7000 cm^{-1} have been recorded by Brenda Winnewisser and co-workers in a study analogous to their work on the spectrum of D_2O.[62,63] These still unpublished data were assigned by us and also used in the fit.

After collecting all the observed data we made a multilayer check of the levels. Comparisons were made with energy levels calculated using the PS PES; checks were made on levels by J, parity, and energy so that we could exclude misassignments and other mistakes from the experimental data. In particular, any level which differed by more than 1 cm^{-1} was regarded as suspicious. At least 200 levels were excluded from the data set for a variety of reasons, leaving 4495 experimental levels with $J\leqslant 10$; the 3478 levels which have $J\leqslant 8$ were used in the fit.

D. The fit

The two sets of data (experimental and *ab initio*) are different in nature. Their compatibility is provided by special weight factors assigned to the experimental ($W_i^{\rm exp}$) and the *ab initio* ($W_i^{\rm ai}$) parts. The ratio parameter $R=W_i^{\rm exp}/W_i^{\rm ai}$ controls the relative importance of the two input data sets. For example, an $R=0$ corresponds to a fitting to the *ab initio* energies only, while for $1/R=0$ the refinement is completely unconstrained, and the surface is adjusted only to the experimental data. An optimal value of $R=100$ was obtained in a linear search as follows. We started the refinement with a small value ($R=0.000\,01$) only fitting to the $HD^{16}O$ $J=0$ levels, see Table I. Then we tried a larger R (0.0001) using the refined potential parameters from the previous step as an input. Continuing this procedure until we reached convergence we arrived at the value $R=100$. Using this value we included in the fittings $J=1$, $J=2$, and so on, each time using obtained f_{ijk} as an input. Finally at the $J=8$ fitting step, which included 3478 experimental levels, we switched again to the linear search of the optimal R value. To our surprise, by gradually improving the overall rms error we arrived at the $1/R=0$ limit, i.e., to an unconstrained fit.

The final potential, which we refer to as HDO_07, reproduces the experimental term values with the rms error of 0.0347 or 0.039 cm^{-1} for only the $J=0$ levels. Term values below 14 000 cm^{-1} that were included in the fitting are well reproduced, typically within 0.02 cm^{-1}, while there are errors of 0.14 cm^{-1} for the stretching band (006) for which 50 levels with $J\leqslant 8$ were included in the fit. Table I compares our vibrational band origins calculated from the HDO_07 PES with results from other potentials and observations. Since the previous studies using the PS potential[15,20,21] are not converged at high energies, the PS results presented in Tables I and II are our own calculation. A full list of predicted band origins, with vibrational assignments, for both the HDO_07 and *ab initio* CVRQD potentials are given in the electronic archive.[64]

Computed term values for $J=3$, $p=0$ levels are listed in Table II; our new surface reproduces the measured values with a standard deviation of 0.03 cm^{-1}. A similar comparison is given in Fig. 1 for the 169 experimental levels with $J=12$, $p=0$. These levels were not used in the original fit; however, the HDO_07 surface predicts these states accurately, giving $\sigma=0.045$ cm^{-1}. It should be noted that for higher J values rotational nonadiabatic effects are expected to become important;[14] these have been neglected in the present study.

The resulting spectroscopic surface shows a rms deviation of 19.5 cm^{-1} from the reference *ab initio* energies, which is illustrated on Figs. 2 and 3 for different molecular geometries. Our best fit parameters f_{ijk} are given as supplemented materials[64] in the form of a FORTRAN program which reproduces our fitted $HD^{16}O$ PES.

It should be noted that although our final fit was uncon-

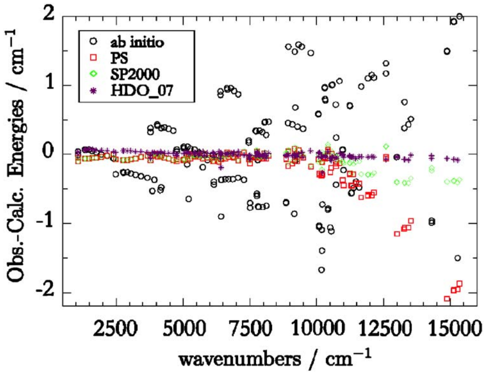

FIG. 1. (Color online) Observed − calculated energies for states with $J=12$, $p=0$ as predicted by the CVRQD *ab initio* potential (Ref. 27) and Partridge and Schwenke's spectroscopic potentials in the original, PS (Ref. 15), and improved, SP2000 (Refs. 20 and 21), calculations, and this work, HDO_07. Experimental levels are from Refs. 38, 52, 54, 57–59, and 66.

strained by the *ab initio* data $(1/R=0)$, it was only by imposing the *ab initio* constraint that we were able to reach this point. Apparently we have found one of the possible minima of the fitting problem we defined, although not necessarily the lowest one. It is difficult to prove that our potential does not suffer from artificial ripples or bulges as a result of the fitting process but our graphical inspection showed no evidence of this behavior, and we believe that our fitting procedure should act to reduce the likelihood of this occuring in spectroscopically important regions of the potential.

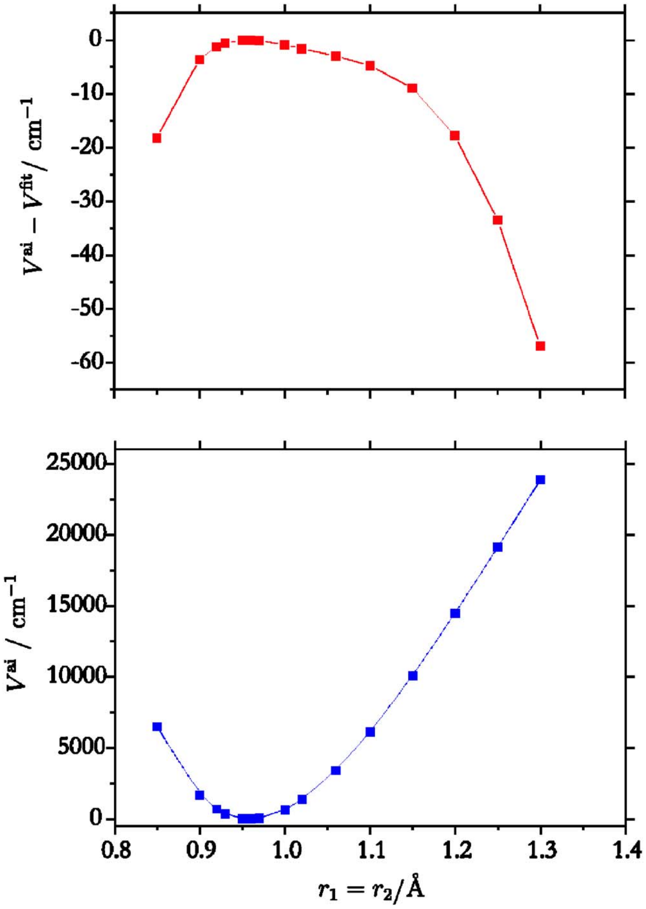

FIG. 2. (Color online) Difference between initial *ab initio* and refined PES (upper panel) along the stretching coordinate $r_1=r_2$. The interbond angle is fixed at $\theta=104°$. The lower panel shows the initial *ab initio* PES.

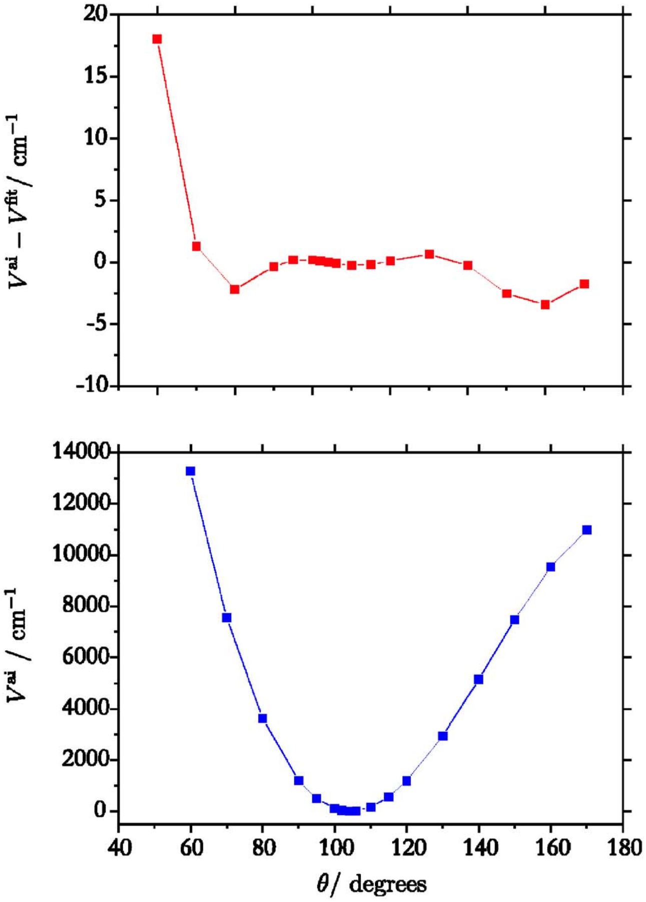

FIG. 3. (Color online) Difference between the initial *ab initio* and refined PES (upper panel) along the bending coordinate θ. The bond lengths are fixed at $r_1=r_2=0.96$ Å. The lower panel shows the initial *ab initio* PES.

III. RESULTS AND COMPARISON WITH PREVIOUS WORK

The standard deviation of 0.035 cm^{-1} for the HDO_07 potential presented here can be compared to 0.45 cm^{-1} for the PS potential[20] and 1.9 cm^{-1} for the CVRQD *ab initio* potential[26,27] for the same data. The maximum and minimum deviations show similar characteristics. Our potential therefore reproduces the observed levels to much higher accuracy, giving the HDO_07 potential a major advantage for both assigning and modeling spectra.

The ability to reproduce the observed energy levels is one important quality of a PES. However, there are other observations sensitive to the PES such as the intensities of vibration-rotation transitions. These are particularly sensitive in regions where there is a resonant interaction between states belonging to two distinct vibrational bands.

Figure 4 illustrates the improvement given by our potential. The upper panel in this figure gives transitions in the Q branch of the (013)-(000) band. This band is mostly isolated and calculations with two distinct spectroscopically determined potentials (Ref. 15 and here) and two distinct *ab initio* dipole moment surfaces[20,29] (DMS) all reproduce the observed intensities satisfactorily. Conversely the lower panel

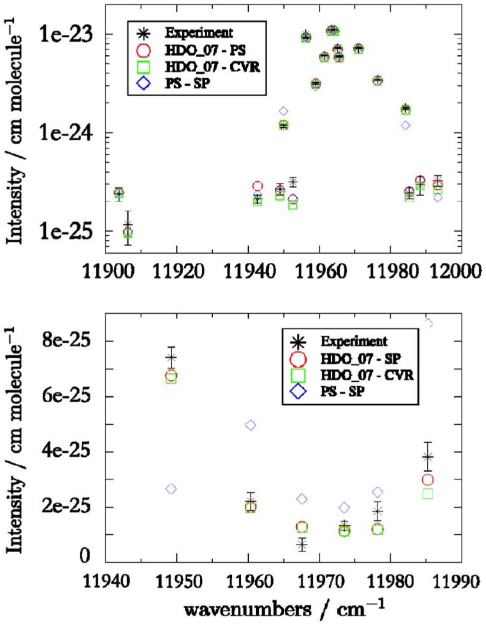

FIG. 4. (Color online) Transition intensities for selected states involving $J=1$, 2, and 3. Experimental data from Refs. 56 and 57. Calculations are labeled using the format PES-DMS, where PS is the surface of Partridge and Schwenke (Ref. 15), HDO_07 is the PES of the present work, SP is the dipole moment surface of Schwenke and Partridge (Ref. 20), and CVR is the DMS of Lodi *et al.* (Ref. 29). Upper panel: 20 *Q*-branch lines of the (013)-(000) band; lower panel six *Q*-branch lines of the (330)-(000) band. This band has a strong resonance with the (013)-(000).

gives the corresponding results for the (330)-(000) band. This band has a strong accidental resonance interaction with the stronger (013)-(000) band. The intensities of transitions with the (330)-(000) band are therefore very sensitive to details of the PES used in their calculation although, as shown in the figure, they are much less sensitive to the precise DMS used. It is clear that our fit reproduces the resonance interactions between these in a significantly more satisfactory manner than the fit of Partridge and Schwenke.[15]

IV. DISCUSSION AND CONCLUSION

We have used 3478 experimentally determined energy levels of $HD^{16}O$ to adjust 113 parameters of an initially *ab initio* potential energy surface. *Ab initio* data were also used to initially constrain this fit, although it was not required for the final iteration, and therefore this procedure can be thought of as a process of guiding the fit toward a (local) minimum, where the fit does not unreasonably distort the potential in regions not constrained by the observed data. It should be noted that during this fit no account was made of the errors in the experimental data although this differs significantly between the energy levels. This was not deemed necessary as the published errors are all smaller than the standard deviation found here. However, this will no longer be true if further significant improvement of the fit is to be made. It would be desirable to perform future fits with energy levels whose errors have been systematically and simultaneously determined.[67] To do this it will be necessary not only to account for statistical errors but also to deal with systematic errors such as the calibration differences between spectra recorded in different laboratories which have recently been found to give shifts as large as 0.01 cm^{-1}.[57]

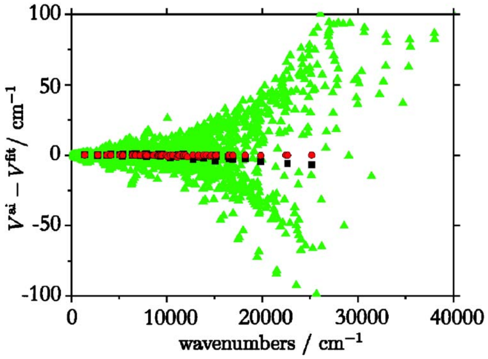

FIG. 5. (Color online) The differences between the initial *ab initio* V^{ai} and refined V^{fit} potential energy surfaces (triangles) plotted against the *ab initio* energy values. The Obs.-Calc. deviations for vibrational term values from Table I are also shown: the squares represent the DVR3D results obtained using the original *ab initio* PES (last column of Table I), whereas the circles indicate results obtained with the refined PES (column 5 of Table I).

In order to improve on the properties of the best available *ab initio* ground electronic state potential energy surface of $HD^{16}O$, we empirically adjust it by fitting to available high resolution observed spectroscopic data for $HD^{16}O$. In this process a standard problem is that there is insufficient experimental data to unambiguously define all the important potential parameters. There are a number of methods of overcoming this problem. The most obvious one is to fix some parameters either to their *ab initio* values or simply to zero. Although such fits usually improve the calculated energies, the constraints can lead to unpredictable, and often unphysical, features in the PES in regions poorly sampled by the experimental data. Another method of reducing the number of fitting parameters is to use a morphing function.[6,68,69] In our approach we impose constraints by requiring the PES to stay close to the *ab initio* surface. In this way we can better control the shape of PES and circumvent a possible shortage of experimental data as they are supplemented by the *ab initio* information.

Although our method of refining a PES is not unique, it results in a very practical method of using spectroscopic data which improves the accuracy of the PES, where it is well studied and retains the predictive properties of the underlying *ab initio* PES. However, we do not claim that our fit improves the *ab initio* surface, i.e., that our spectroscopic surface is closer to the "true" PES of $HD^{16}O$, in regions which are not probed by the available spectroscopic data. In order to illustrate this point Fig. 5 shows the deviations $V^{ai}-V^{fit}$ for all 2000 energy grid points, where V^{fit} denotes the refined potential surface. On the same plot we show the Obs.-Calc. deviations for the $J=0$ term values from Table I computed both from the original *ab initio* PES and from our new PES. If we used only the latter information to assess the quality of surfaces, the spectroscopic PES would seem only about 0.1 cm^{-1} away from the true PES of $HD^{16}O$, while the *ab initio* PES is within 5–6 cm^{-1}. However, the scattering $V^{ai}-V^{fit}$ indicates that the actual range of accuracy is essentially larger. It is possible that a different analytical representation could provide better physical properties of the refinement. More extensive and accurate *ab initio* data would be also a great help.

ACKNOWLEDGMENTS

We thank Brenda Winneswisser for supplying her unpublished data. This work was supported by the European Commission through Contract No. HPRN-CT-2000-00022 "Spectroscopy of Highly Excited Rovibrational States" and Contract No. MRTN-CT-2004-512202 "Quantitative Spectroscopy for Atmospheric and Astrophysical Research" and through a Marie Curie Incoming Fellowship to B.A.V. It was also supported by the UK National Environmental Research Council (NERC) and INTAS. The study was performed as part of IUPAC task group 2004-035-1-100 "A database of water transitions from experiment and theory."

[1] L. S. Rothman, D. Jacquemart, A. Barbe, D. Chris Benner, M. Birk, L. R. Brown, M. R. Carleer, C. Chackerian, Jr., K. Chance, L. H. Coudert, V. Dana, V. M. Devi, J.-M. Flaud, R. R. Gamache, A. Goldman, J.-M. Hartmann, K. W. Jucks, A. G. Maki, J.-Y. Mandin, S. T. Massie, J. Orphal, A. Perrin, C. P. Rinsland, M. A. H. Smith, J. Tennyson, R. N. Tolchenov, R. A. Toth, J. Vander Auwera, P. Varanasi, and G. Wagner, J. Quant. Spectrosc. Radiat. Transf. **96**, 139 (2005).

[2] V. E. Zuev and V. S. Komarov, *Statistical Models of the Temperature and Gaseous Components of the Atmosphere* (Reidel, Dordrecht, 1988).

[3] R. C. M. Learner, W. Zhong, J. D. Haigh, D. Belmiloud, and J. Clarke, Geophys. Res. Lett. **26**, 3609 (1999).

[4] B. A. Voronin, I. M. Nasrtdinov, A. B. Serebrennikov, and T. Y. Chesnokova, Atmos. Oceanic Opt. **16**, 272 (2003).

[5] I. V. Ptashnik and K. P. Shine, Atmos. Oceanic Opt. **16**, 251 (2003).

[6] S. V. Shirin, O. L. Polyansky, N. F. Zobov, P. Barletta, and J. Tennyson, J. Chem. Phys. **118**, 2124 (2003).

[7] J. A. Fernley, S. Miller, and J. Tennyson, J. Mol. Spectrosc. **150**, 597 (1991).

[8] C. D. Paulse and J. Tennyson, J. Mol. Spectrosc. **168**, 313 (1994).

[9] O. L. Polyansky, P. Jensen, and J. Tennyson, J. Chem. Phys. **101**, 7651 (1994).

[10] O. L. Polyansky, P. Jensen, and J. Tennyson, J. Chem. Phys. **105**, 6490 (1996).

[11] J. H. Schryber, O. L. Polyansky, P. Jensen, and J. Tennyson, J. Mol. Spectrosc. **185**, 234 (1997).

[12] J. S. Kain, O. L. Polyansky, and J. Tennyson, Chem. Phys. Lett. **317**, 365 (2000).

[13] H. M. Quiney, P. Barletta, G. Tarczay, A. G. Császár, O. L. Polyansky, and J. Tennyson, Chem. Phys. Lett. **344**, 413 (2001).

[14] S. V. Shirin, O. L. Polyansky, N. F. Zobov, A. G. Császár, and J. Tennyson, J. Mol. Spectrosc. **236**, 216 (2006).

[15] H. Partridge and D. W. Schwenke, J. Chem. Phys. **106**, 4618 (1997).

[16] A. J. C. Varandas, A. I. Voronin, and P. J. S. B. Caridade, J. Chem. Phys. **108**, 7623 (1998).

[17] J. Brandao and C. M. A. Rio, J. Chem. Phys. **119**, 3148 (2003).

[18] N. F. Zobov, O. L. Polyansky, C. R. Le Sueur, and J. Tennyson, Chem. Phys. Lett. **260**, 381 (1996).

[19] D. W. Schwenke, J. Phys. Chem. A **105**, 2352 (2001).

[20] D. W. Schwenke and H. Partridge, J. Chem. Phys. **113**, 6592 (2000).

[21] O. Naumenko, E. Bertseva, A. Campargue, and D. W. Schwenke, J. Mol. Spectrosc. **201**, 297 (2000).

[22] P. Theule, A. Callegari, and T. Rizzo, J. Chem. Phys. **122**, 124312 (2005).

[23] A. Jenouvrier, M. F. Marienne, M. Carleer, R. Colin, A.-C. Vandaele, P. F. Bernath, O. L. Polyansky, and J. Tennyson, J. Mol. Spectrosc. **209**, 165 (2001).

[24] J. Tennyson, G. J. Harris, R. J. Barber, S. La Delfa, B. Voronin, and Y. V. Pavlenko, Mol. Phys. **105**, 701 (2007).

[25] J. Tennyson, Phys. Scr. **76**, C53 (2006).

[26] O. L. Polyansky, A. G. Császár, S. V. Shirin, N. F. Zobov, P. Barletta, J. Tennyson, D. W. Schwenke, and P. J. Knowles, Science **299**, 539 (2003).

[27] P. Barletta, J. Tennyson, S. V. Shirin, N. F. Zobov, O. L. Polyansky, E. F. Valeev, and A. G. Császár, J. Chem. Phys. **125**, 204307 (2006).

[28] A. G. Császár, G. Czakó, T. Furtenbacher, J. Tennyson, V. Szalay, S. V. Shirin, N. F. Zobov, and O. L. Polyansky, J. Chem. Phys. **122**, 214205 (2005).

[29] L. Lodi, R. N. Tolchenov, J. Tennyson, A. E. Lynas-Gray, S. V. Shirin, N. F. Zobov, O. L. Polyansky, A. G. Császár, J. van Stralen, and L. Visscher, "A new *ab initio* ground state dipole moment surface for the water molecule," J. Chem. Phys. (to be published).

[30] S. N. Yurchenko, M. Carvajal, P. Jensen, F. Herregodts, and T. R. Huet, Chem. Phys. **290**, 59 (2003).

[31] S. N. Yurchenko, P. R. Bunker, W. P. Kraemer, and P. Jensen, Can. J. Chem. **82**, 694 (2004).

[32] S. N. Yurchenko, J. Breidung, and W. Thiel, Theor. Chem. Acc. **114**, 333 (2005).

[33] S. N. Yurchenko, H. Lin, J. J. Zheng, P. Jensen, and W. Thiel, J. Chem. Phys. **123**, 134308 (2004).

[34] R. P. Feynman, Phys. Rev. **56**, 340 (1939).

[35] J. Tennyson, M. A. Kostin, P. Barletta, G. J. Harris, J. Ramanlal, O. L. Polyansky, and N. F. Zobov, Comput. Phys. Commun. **163**, 85 (2004).

[36] J. Tennyson and B. T. Sutcliffe, J. Chem. Phys. **77**, 4061 (1982).

[37] R. J. Barber, J. Tennyson, G. J. Harris, and R. N. Tolchenov, Mon. Not. R. Astron. Soc. **368**, 1087 (2006).

[38] R. A. Toth, http://mark4sun.jpl.nasa.gov/data/spec/H2O (2006).

[39] R. A. Toth, J. Mol. Spectrosc. **195**, 73 (1999).

[40] R. A. Toth and J. W. Brault, Appl. Opt. **22**, 908 (1983).

[41] R. A. Toth, J. Mol. Spectrosc. **186**, 66 (1997).

[42] R. A. Toth, J. Mol. Spectrosc. **162**, 20 (1993).

[43] R. A. Toth, J. Mol. Spectrosc. **186**, 276 (1997).

[44] R. A. Toth, V. D. Gupta, and J. W. Brault, Appl. Opt. **21**, 3337 (1982).

[45] T. Parekunnel, F. Bernath, N. F. Zobov, S. V. Shirin, O. L. Polyansky, and J. Tennyson, J. Mol. Spectrosc. **101**, 28 (2001).

[46] O. N. Ulenikov, S.-M. Hu, E. S. Bekhtereva, G. A. Onopenko, X. Wang, S.-G. He, J.-J. Zheng, and Q.-S. Zhu, J. Mol. Spectrosc. **208**, 224 (2001).

[47] P. Macko, D. Romanini, S. N. Mikhailenko, O. V. Naumenko, S. Kassi, A. Jenouvrier, V. G. Tyuterev, and A. Campargue, J. Mol. Spectrosc. **227**, 90 (2004).

[48] O. Naumenko, E. Bertseva, and A. Campargue, J. Mol. Spectrosc. **197**, 122 (1999).

[49] O. Naumenko and A. Campargue, J. Mol. Spectrosc. **199**, 59 (2000).

[50] E. Bertseva, O. Naumenko, and A. Campargue, J. Mol. Spectrosc. **203**, 28 (2000).

[51] O. Naumenko, E. Bertseva, and A. Campargue, J. Mol. Spectrosc. **204**, 94 (2000).

[52] E. Bertseva, O. Naumenko, and A. Campargue, J. Mol. Spectrosc. **221**, 38 (2003).

[53] O. Naumenko and A. Campargue, J. Mol. Spectrosc. **221**, 221 (2003).

[54] O. Naumenko, S. M. Hu, S. G. He, and A. Campargue, Phys. Chem. Chem. Phys. **6**, 910 (2003).

[55] A. Campargue, I. Vasilenko, and O. Naumenko, J. Mol. Spectrosc. **234**, 216 (2005).

[56] M. Bach, S. Fally, P.-F. Coheur, M. C. A. Jenouvrier, and A. C. Vandaele, J. Mol. Spectrosc. **232**, 341 (2005).

[57] B. A. Voronin, O. V. Naumenko, R. N. Tolchenov, J. Tennyson, S. Folly, P.-F. Coheur, M. Carleer, A. Jenouvrier, and A. C. Vandaele, J. Mol. Spectrosc. **244**, 87 (2007).

[58] O. Naumenko, S. Voronina, and S.-M. Hu, J. Mol. Spectrosc. **227**, 151 (2004).

[59] S.-M. Hu, O. N. Ulenikov, E. S. Bekhtereva, S.-G. He, X. Wang, H. Lin, and Q.-S. Zhu, J. Mol. Spectrosc. **203**, 228 (2000).

[60] S. Hu, H. Lin, S. He, J. Cheng, and Q. Zhu, Phys. Chem. Chem. Phys. **1**, 3727 (1999).

[61] A. Callegari, P. Theule, R. N. Tolchenov, N. F. Zobov, O. L. Polyansky, J. Tennyson, J. S. Muenter, and T. R. Rizzo, Science **297**, 993 (2002).

[62] A. D. Bykov, O. V. Naumenko, L. N. Sinitsa, B. P. Winnewisser, M. Winnewisser, P. S. Ormsby, and K. N. Rao, J. Mol. Spectrosc. **166**, 169 (1994).

[63] P. S. Ormsby, K. N. Rao, M. Winnewisser, B. P. Winnewisser, O. V. Naumenko, A. D. Bykov, and L. N. Sinitsa, J. Mol. Spectrosc. **158**, 109 (1993).

[64] See EPAPS Document No. E-JCPSA6-127-031744 for electronic versions of the HDO_07 potential energy surface as a FORTRAN subroutine plus a file containing all assigned $J=0$ levels. This document can be reached through a direct link in the online article's HTML reference section or via the EPAPS homepage (http://www.aip.org/pubservs/epaps.html).

[65] O. N. Ulenikov, S.-M. Hu, E. S. Bekhtereva, and Q.-S. Zhu, J. Mol. Spectrosc. **231**, 57 (2005).
[66] O. Naumenko, O. Leshichina, and A. Campargue, J. Mol. Spectrosc. **234**, 58 (2006).
[67] T. Furtenbacher, A. G. Császár, and J. Tennyson, J. Mol. Spectrosc. **245**, 115 (2007).
[68] B. Gazdy and J. M. Bowman, J. Chem. Phys. **95**, 6309 (1991).
[69] M. Meuwly and J. M. Hutson, J. Chem. Phys. **110**, 8338 (1999).